Introduction to QSO Absorption Lines

1 Historical Perspective

1.1 Discovery of QSOs

In the 1950s Cambridge radio surveys began to uncover many radio sources all over the sky (i.e. no preference for Galactic coordinates), and originally these were thought to be some sort of radio star in the halo. However, no optical counterparts were known. In 1963, three papers appeared in Nature with the first reports on the nature of these radio stars by studying 3C273.

1. Hazard, Mackey & Shimmins used lunar occultations of the radio source to obtain an accurate position. Find it coincident with a 13th magnitude star-like object.

2. Schmidt took a spectrum of the 'star' and found it to be highly redshifted to $z = 0.158$.

3. Oke found that the spectral energy distribution was a power law, not a black body.

It was therefore clear that these were not stars at all, so they were re-named quasi-stellar objects, or QSOs. However, there was still a debate about whether the redshift was due to Doppler or gravitational redshifts. One piece of evidence against the former was that the energy required far exceeded anything that could be produced through well understood nuclear processes. We now understand QSOs to be one of the family of active galactic nuclei (AGN) which also include low luminosity Seyfert galaxies, and blazars. Although the first QSOs were found with radio surveys, only some 10% are actually radio-loud. Most optical surveys found QSOs through colour selection since they had a UV excess.

By 1966 the record-holder had $z > 2$ and absorption lines were being identified, e.g. Bahcall, Peterson & Schneider (1966). In 1971, Lynds studied the then highest redshift QSO $z = 2.87$ and found numerous absorption clouds bluewards of Lyα emission. He speculated that this was due to abundant intervening HI.

1.2 Absorption Lines - Intervening or Ejected?

Controversial issue - were QALs associated with intervening or associated material? If associated, the ejection velocities are huge (note that we use the Doppler formula with relativistic correction):

$$\beta = \frac{v_{ej}}{c} = \frac{(1+z_e)^2 - (1+z_a)^2}{(1+z_e)^2 + (1+z_a)^2} \tag{1}$$

Values of $\beta > 0.1$ readily observed, but this requires huge amounts of energy. And yet, the Doppler parameters stay small $\sim 10s$ km/s. Big contrast with BALs.

What do the students think? Three key observations resolved the controversy in the 1980s.

1. Line statistics in a homogeneous dataset. Young et al (1980) showed

   - Same line density from QSO to QSO

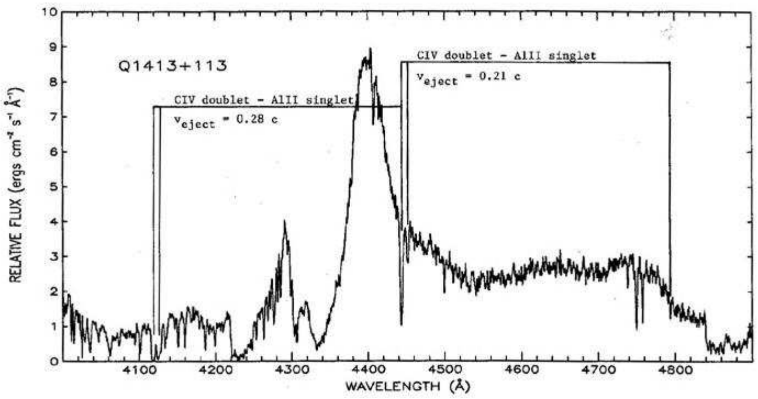

Figure 1:

- Line density not a function of velocity from QSO
- EW distribution same from QSO to QSO
- EW distribution not a function of velocity from QSO
- No difference between lines from continuum ($R \sim 10^{17}$ cm) and BLR ($R \sim 10^{20}$ cm)

2. Association with Galaxies. Boksenberg & Sargent (1978) found CaII absorption due to a $z = 0.005$ galaxy in spectrum of $z = 0.5$ QSO.

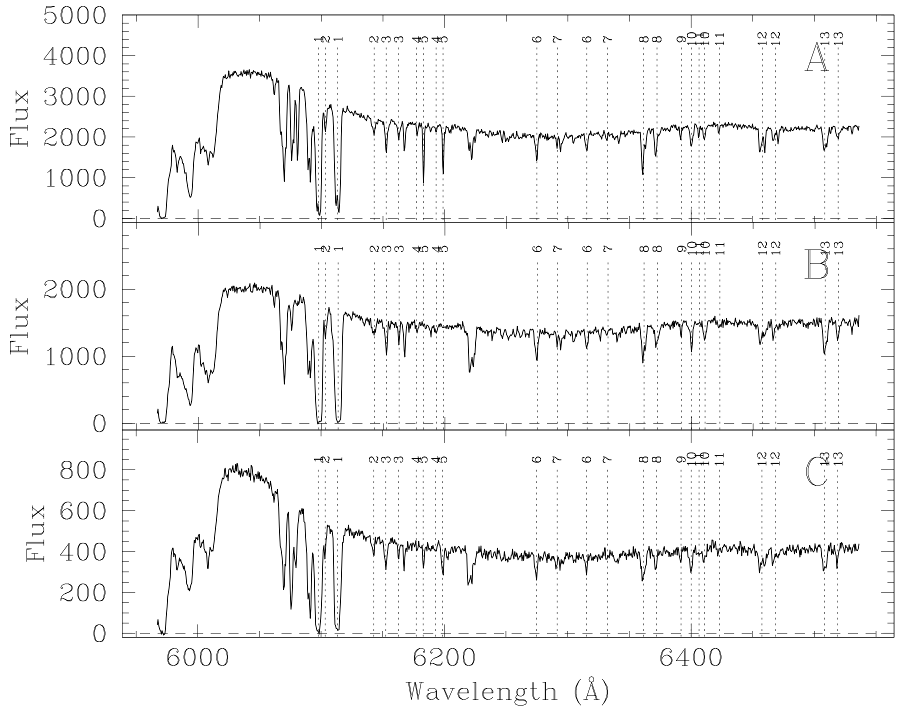

Figure 2:

3. Sizes of Lyα clouds measured by looking at QSO pairs. Found large sizes (Mpc).

Now generally accepted that QALs are probes of intervening matter, although people still wary of proximate systems in case they are associated with or have been affected by the QSO.

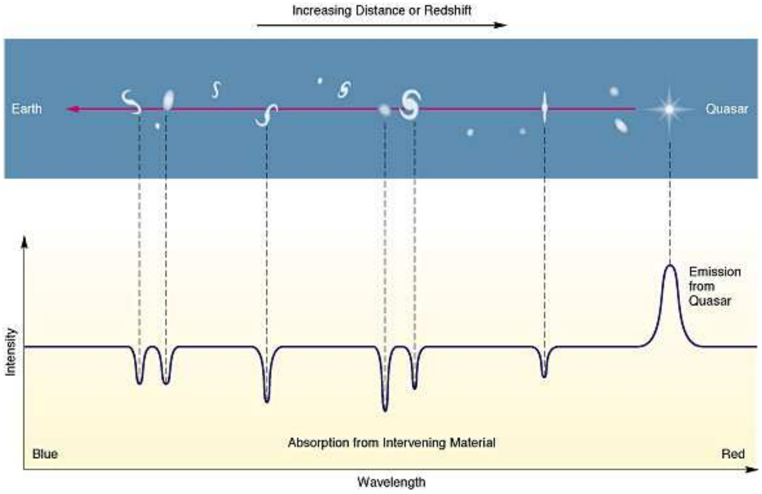

Figure 3:

2 Taxonomy

Absorption lines usually named after the line which primarily identifies them - this can be confusing! However, there are likely some physical differences between these varieties, mostly the impact parameter at which they intersect the intervening galaxy.

There is also a characteristic N(HI) associated with these different systems. Remember, column density is measured in atoms/cm^2.

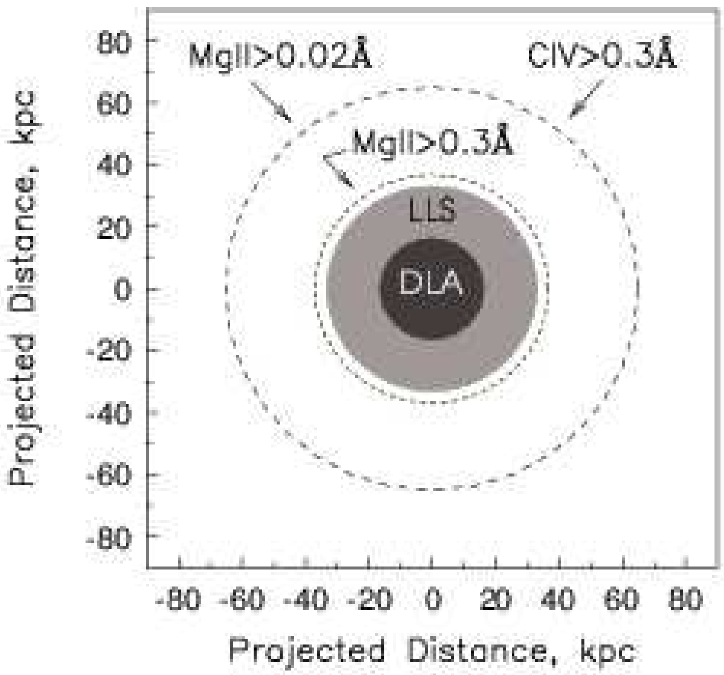

MgII>0.02Å
CIV>0.3Å
MgII>0.3Å
LLS
DLA
80
60
40
20
0
-20
-40
-60
-80
Projected Distance, kpc
-80 -60 -40 -20 0 20 40 60 80
Projected Distance, kpc

Figure 4:

System type	log N(H I)	Spectral signature	Associated with	References
Lyα forest	$\gtrsim$ 11.0	Lyα $\lambda_0 = 1215.67$ Å	IGM	Rauch (1998)
Mg II systems	$\gtrsim$ 17.0	Mg II $\lambda_0 = 2796, 2803$ Å	galactic halo 20 – 40 kpc h_{100}^{-1}	Steidel (1995), Churchill & Carlton (1999)
Lyman limit systems	$\gtrsim$ 17.5	912 Å break	Similar to Mg II systems	Tytler (1982), Lanzetta et al (1995)
Damped Lyα systems	$\gtrsim$ 20.3	Lyα $\lambda_0 = 1215.67$ Å	proto-galaxy	Wolfe (1988), Lanzetta et al (1995)

Table 1: Summary of absorption line systems and their column density classifications.

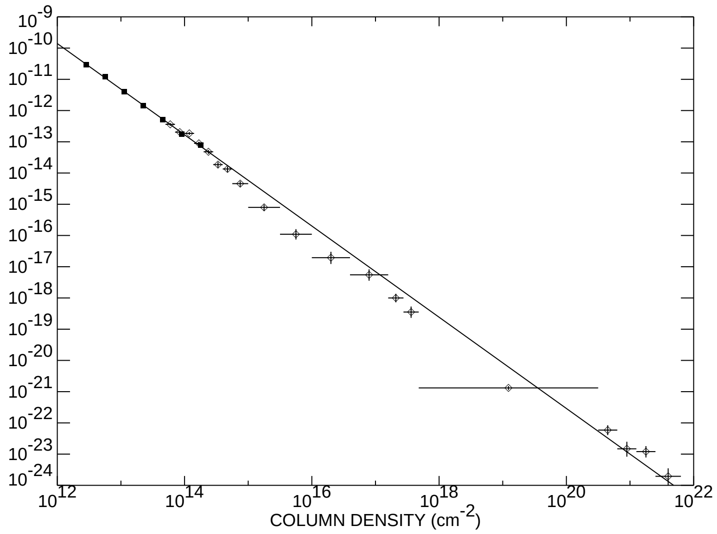

Figure 5:

The column density distribution function is a power law

$$f(N,z)dNdX = \frac{n\ dN\ dX}{\Delta N\ \Delta X} \tag{2}$$

This is the number of systems per unit column density per redshift path interval. This latter quantity, ΔX is closely related to redshift, but takes the expansion of the universe into account, i.e. converts redshift into co-moving coordinates.

$$X(z) = \int_0^z (1+z)^2[(1+z)^2(1+z\Omega_M) - z(2+z)\Omega_\Lambda]^{-1/2}dz \tag{3}$$

If $\Omega_\Lambda = 0$ and $\Omega_M = 0$

$$X(z) = 1/2[(1+z)^2 - 1] \tag{4}$$

If $\Omega_\Lambda = 0$ and $\Omega_M = 1$

$$X(z) = 2/3[(1+z)^{3/2} - 1] \tag{5}$$

The observed CDDF is very close to a power law

$$f(N) = \alpha N^{-\beta} \tag{6}$$

Kim et al (2002) show the latest UVES data fit with $\alpha = 4.9 \times 10^7$ and $\beta = 1.46$. Let's see how this works with an example:

How many absorbers with column densities between $10^{13.75}$ and $10^{14.25}$ between z=3 and z=4?

$z = 3 \quad \rightarrow X = 4.62$ and $z = 4 \quad \rightarrow X = 6.72$ for $\Omega_M = 1$, i.e. $\Delta X = 2.10$. So number of absorbers is

$$n = \alpha N^{-\beta} \times \Delta N \Delta X = 4.9 \times 10^7 \times (10^{14})^{-1.46} \times (10^{14.25} - 10^{13.75}) \times 2.10 \sim 45 \tag{7}$$

The mean N(HI) in a given interval is simply

$$< N(HI) >= \frac{\int_{Nmin}^{Nmax} N.f(N)dN}{\int_{Nmin}^{Nmax} f(N)dN} \tag{8}$$

We can also measure the number density of absorbers, $n(z)$ or dN/dz as the number of systems per unit redshift. This can be written down based on geometrical cross-sections, taking into account the expansion of the universe:

$$n(z) = \frac{cn_0\sigma(z)}{H_0}\frac{1+z}{(1+q_0z)^{1/2}} \tag{9}$$

For non-evolving systems (number and cross-sectional area constant with time)

$$n(z) = n_0(z)(1+z)(1+2q_0z)^{-1/2} \tag{10}$$

Observationally, we determine a line density which is written in the form

$$n(z) = n_0(1+z)^{\gamma} \tag{11}$$

For a non-evolving population $\gamma = 0.5, 1$ for $q_0 = 0.5, 0$.

Note that we expect the number density of absorbers to decrease at low redshift due to the expansion of the universe. By simply counting lines we can determine whether or not the population is evolving, at least whether the product of the cross-section and number is evolving. Can not determine the number AND size, so assume present day galaxy volume density and luminosity function and deduce sizes. Assuming spherical halos (πR^2 replaces $n_0\sigma(z)$ term):

$$n(z) = c/H_0(1+z)(1+2q_0z)^{-1/2} \times \int_0^{\infty} \epsilon\Phi(L)\kappa\pi R^2(L)dL \tag{12}$$

where ϵ is the fraction of galaxies which have halos with HI filling factor κ. We will substitute the Schechter luminosity function: a power law at the faint end with a knee and exponential turnover at high L (which is basically a Gaussian-like distribution of ellipticals). The position of the knee is governed by the empirically determined slope (α) and $L_\star$. The normalization is set by $\Phi_\star$:

$$\Phi(L/L_*) = \Phi_*(L/L_*)^{-\alpha}exp(-L/L_*) \tag{13}$$

Also substitute the Holmberg relation (R_* is the Holmberg radius, the galaxy size at 26.5 mags/arcsec^2), another scaling relation between luminosity and size:

$$\frac{R}{R_*} = (\frac{L}{L_*})^{\beta} \tag{14}$$

We can use the LF and the Holmberg relation to determine R_*, a scaling length for DLAs

$$\frac{1}{R_*^2} = \frac{c(1+z)(1+2q_0z)^{-1/2}}{H_0n(z)} \times \epsilon\Phi_*\kappa\pi\Gamma(1+2\beta-\alpha) \tag{15}$$

Using the values

$\epsilon = \kappa = 1$
$\beta = 0.4$

$\alpha = 1.25$
$\Phi_* = 1.4 \times 10^{-2} h^3 Mpc^{-3}$

$$R_* = 59 h_{100}^{-1} (\frac{n(z)}{(1+z)})^{1/2} \times (1 + 2q_0 z)^{1/4} \quad \text{kpc} \tag{16}$$

i.e. DLAs are galaxy scale absorbers.

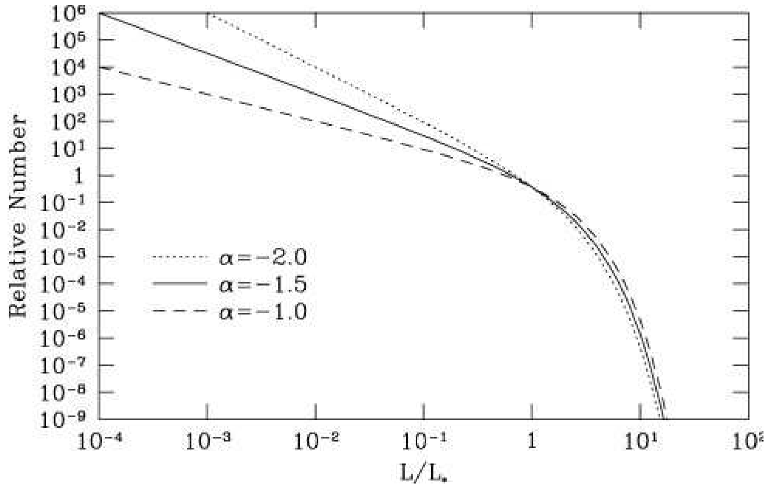

Figure 6: Schechter luminosity function - power law with exponential drop-off at high L.

2.1 Lyα Forest

Now understood that these lines arise in the IGM, more detail on this next lecture. Due to the slope of f(N), the Lyα forest clouds are the most abundant and, in fact, are the main reservoir for baryons at high z. We see absorption from neutral HI, but the majority of the IGM is ionized, else we'd see a GP trough.

2.2 Damped Lyman Alpha Systems

Highest column density systems N(HI)$\geq 2 \times 10^{20}$ atoms/cm^2 associated with galaxy scale absorbers. We'll look at these in detail in a future lecture.

2.3 MgII Systems

These were the first 'types' of absorber to be associated with galaxies in large numbers. In the early 1990s Steidel and Dickinson undertook large surveys of Mg II systems and went looking for the galaxy counterparts. Their main results were

1. One-to-one correspondence between absorbers and galaxies i.e. few galaxies close to QSO don't cause absorption.

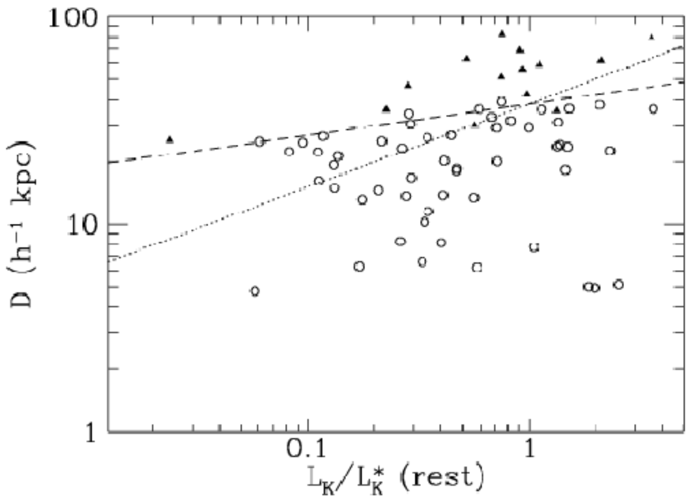

Figure 7: Open circles - galaxies with absorbers. Filled triangles - galaxies with no absorbers. Sizes scale as R(L) = 35 kpc $(L/L_*)^{0.2}$ (dashed line).

2. Normal field galaxies with $L > 0.05L_*$ are potentially galaxy absorbers.

3. The typical Mg II absorber is a $0.7L_*$ Sb galaxy

4. Mg II absorption occurs in a roughly spherical halo with size $\sim 30 - 40$ kpc.

However, there is evidence that individual 'clouds' inside the halos might have much smaller sizes. This is inferred from closely separated multiple lines of sight through gravitationally lensed QSOs. Compare EWs in CIV and MgII systems.

Can use a maximum likelihood technique to infer mostly likely radius of MgII absorber, find $\sim$ 2 kpc.

At least some of the absorption seems to be in the disk, but not all.

Finally, we note that MgII systems are a handy way of pre-selecting DLAs at low redshift when no HI is available.

2.4 Lyman Limit Systems

A LLS is any absorber with a high enough N(HI) to be optically thick at the Lyman limit (912 Å). This corresponds roughly to log N(HI) $\sim$ 17. All DLAs are, by definition, LLSs, as are all MgII systems. Note that LBGs are picked by this spectral feature.

2.5 CIV Systems

- Trace gas that is more highly ionized than Mg II systems.
- Velocity structure of gas is different from neutral species.
- Can be detected down to very low HI column densities.

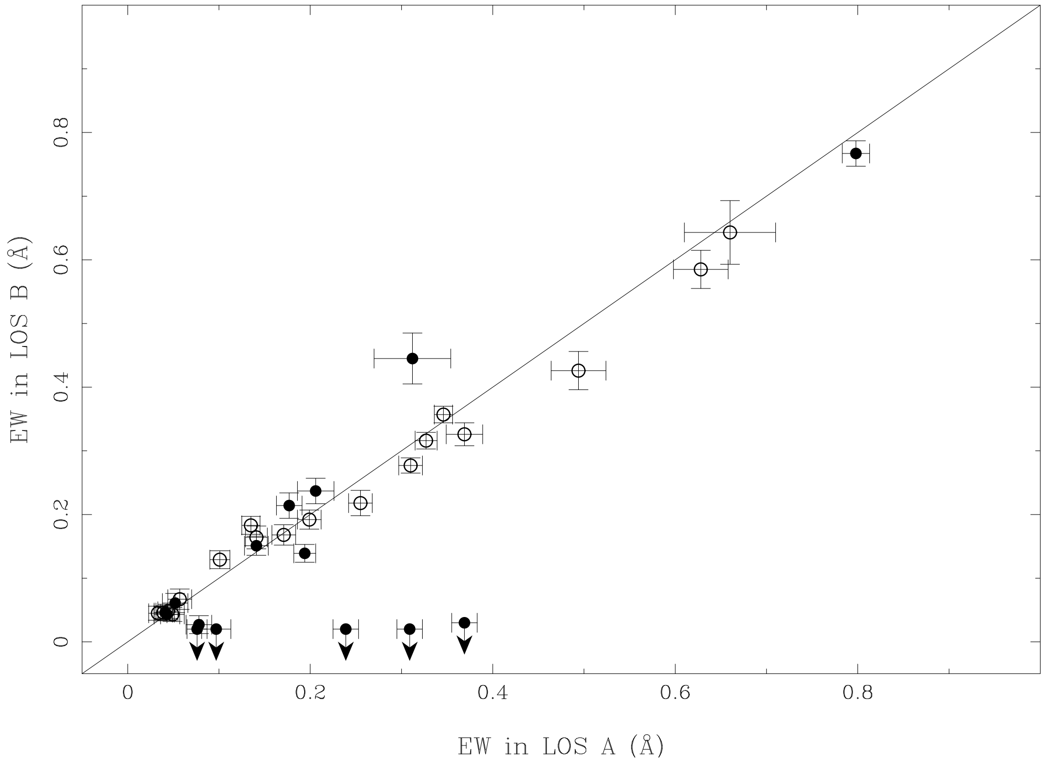

Figure 8: Solid points are MgII, open points are CIV

- Some are probably associated with galaxy halos, others may be truly intergalactic.

CIV systems are very numerous, and their CDDF doesn't show any sign of a turnover. We'll return to this ubiquity in the lecture on the Lyα forest.

Two pieces of evidence that CIV systems are large.

1. Multiple lines of sight find coherence on scales approaching 100 kpc
2. Correlation between LBGs and CIV absorbers out to $\sim$ 200 kpc.

3 Instrumentation

An absorption line can be described by 3 quantities:

1. Redshift: This governs the observed wavelength of a given line, $\lambda_{obs} = \lambda_{rest} \times (1 + z)$.
2. Column density: This relates to the observed EW (non-degenerately in the weak and damped regimes of the COG)
3. Doppler width (b-value): One measure of the line width (others are FWHM and σ).

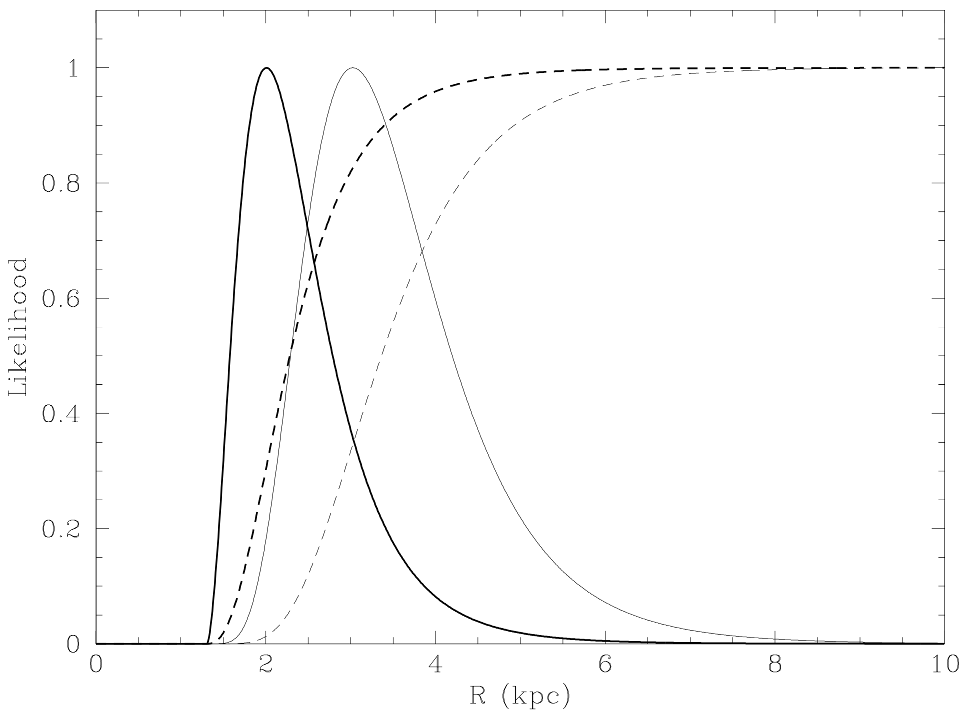

Figure 9: Maximum likelihood test for MgII sizes

As we have previously seen, the resolution of the spectrograph (i.e. the number of pixels over which an infinitely narrow line will be sampled) is related to the detection limit. Resolution is also important if we want to determine accurately the b-value and check that the line is not saturated. Typical b-values for QALs are 5–20 km/s, so high resolution is required.

In a normal spectrograph there is a trade off between wavelength coverage and resolution. In order to obtain both, we use a cross-dispersed echelle spectrograph. Consider the basic equation for a reflection grating with groove spacing $a = 1/n$ (i.e. n lines per length)

$$m\lambda = a(sin\beta + sin\alpha) \tag{17}$$

α is the angle of incidence and β is the angle through which the mth order is reflected.

The angular dispersion can be calculated by keeping α constant and differentiating wrt λ

$$\text{Resolution} \equiv \frac{\mathrm{d}\beta}{\mathrm{d}\lambda} = \frac{\mathrm{m}}{\mathrm{a}\ \cos\beta} = \frac{\sin\beta + \sin\alpha}{\lambda\cos\beta} \tag{18}$$

A high spatial resolution can therefore be achieved by working at high orders and with large angles of incidence and reflection. For a given set of α and β the grating equation is satisified at all wavelengths where m is an integer. As a result successive orders contain a superposition of wavelengths reflected through the same angle causing confusion. I.e.

$$m\lambda' = (m+1)\lambda \tag{19}$$

In long slit work, this is usually undesirable and a blocking (or order-sorting) filter is used to block $m > 1$ light (although sometimes people work in $m > 1$ in order to get high resolution). In

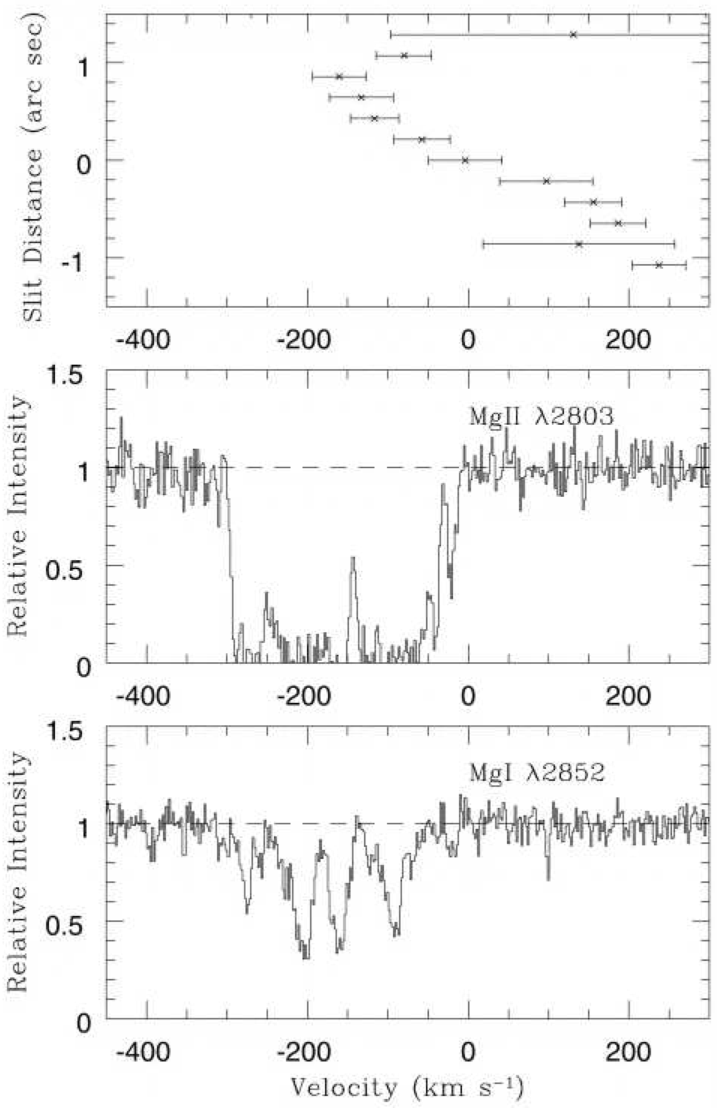

Figure 10:

an echelle, a cross-disperser is placed at 90 degrees to the original dispersing element to separate the orders. This results in many orders on the same CCD. The free spectral range (FSR) is the wavelength range covered uniquely by a given order and is defined as

$$\Delta\lambda = \lambda' - \lambda = \lambda/m \tag{20}$$

The FSR is therefore small for shorter wavelengths. Gaps are often introduced in the wavelength coverage because CCDs are too small to cover the entire FSR of the redder orders. You can change the echelle angle or cross disperser angles to cover the wavelengths that you want; changing the echelle angle effectively shifts the CCD horizontally and changing the XD angle shifts vertically.

Typical resolution of echelles such as HIRES on Keck or UVES on the VLT is

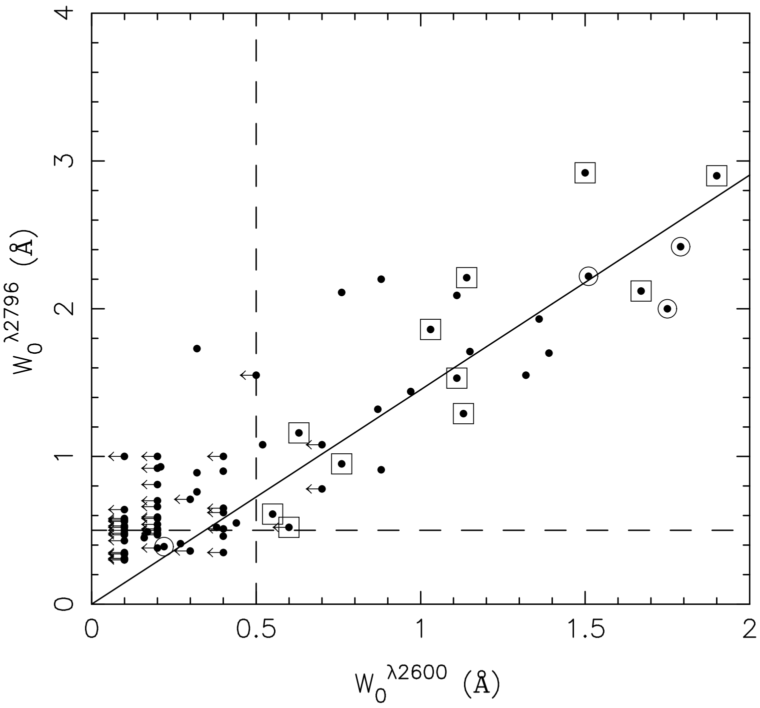

Figure 11:

$$R = \frac{\lambda}{\Delta\lambda(FWHM)} \sim 50,000 \tag{21}$$

Equivalently, this is around 6 km/s.

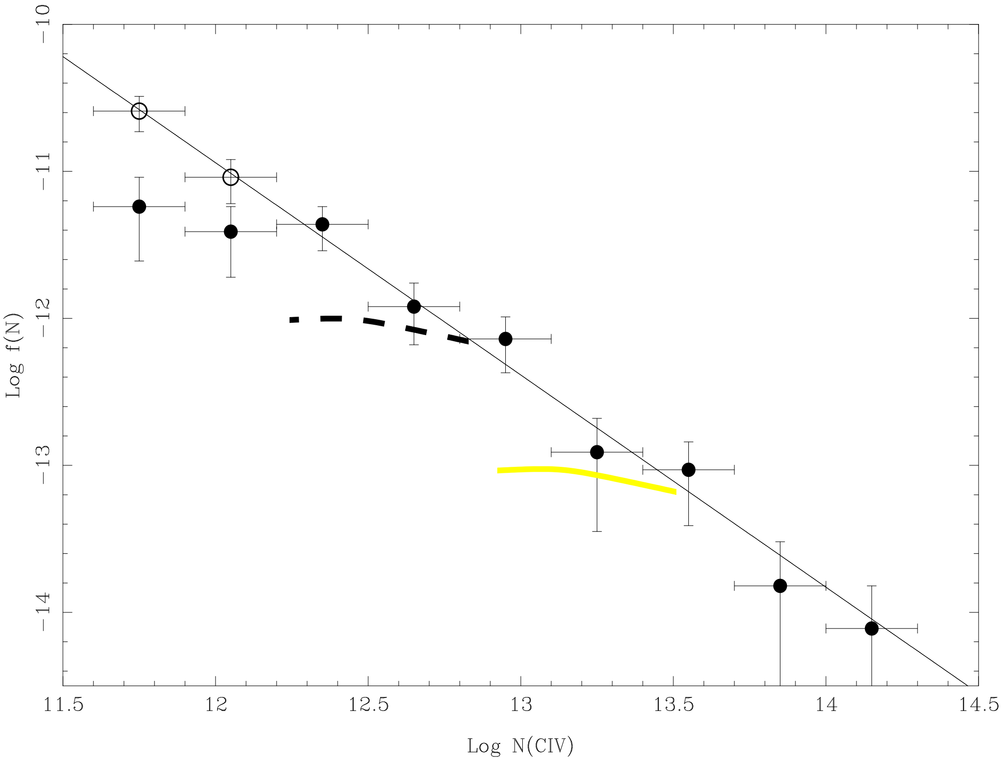

Figure 12:

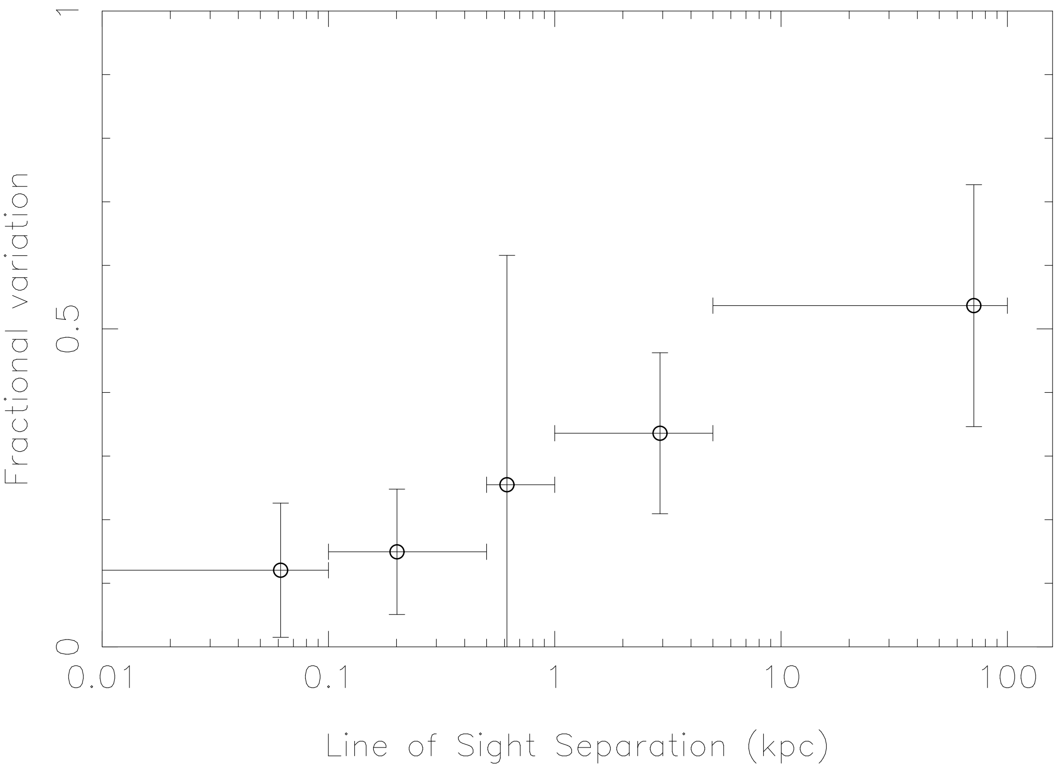

Figure 13: Fractional change in CIV EWs as a function of linear separation in lensed QSOs

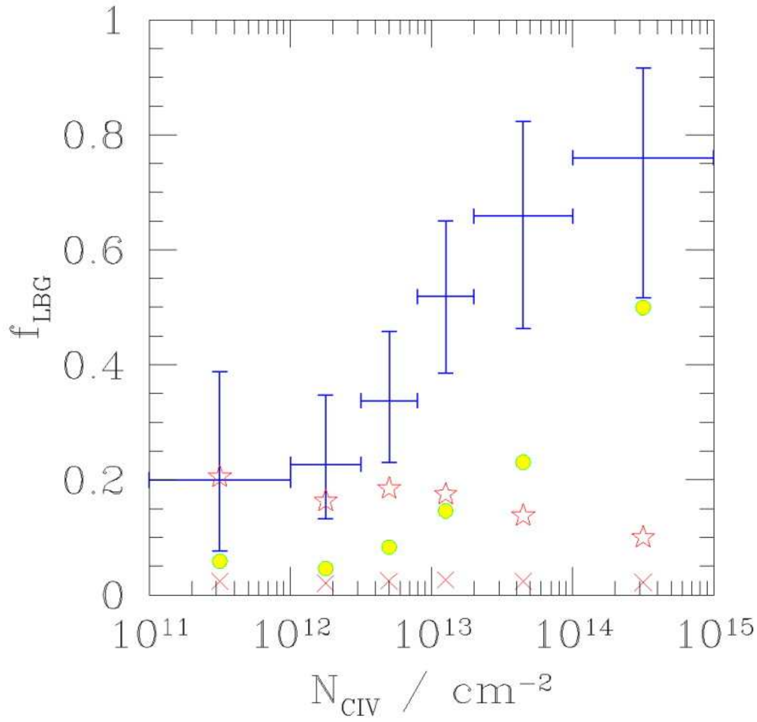

Figure 14: Fraction of CIV systems of a given N(CIV) that lie within 250 kpc of LBG. Small red crosses show expectation for random associations.

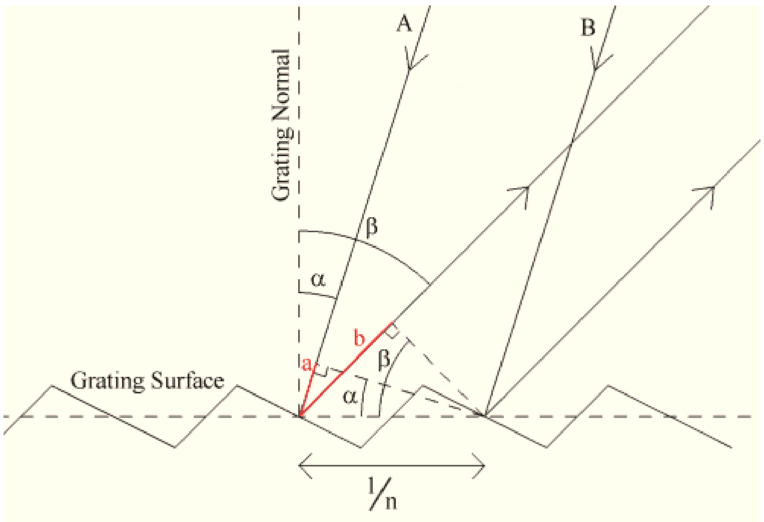

Figure 15: Reflection grating.